AD-A091 388 SACLANT ASW RESEARCH CENTRE LA SPEZIA (ITALY) F/G 17/1
A METHOD OF REDUCING BEARING ERRORS IN HORIZONTAL LINEAR HYDROP--ETC(U)
SEP 80 R KLEMM
UNCLASSIFIED SACLANTCEN-SR-40 NL

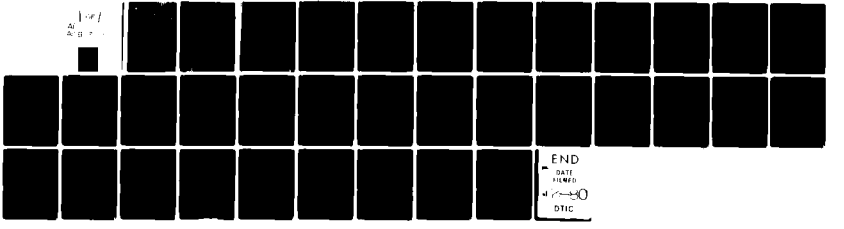

SACLANTCEN Report
SR - 40

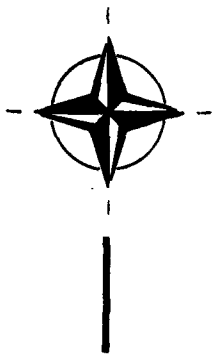

LEVEL II

SACLANT ASW
RESEARCH CENTRE
REPORT

A METHOD OF REDUCING BEARING ERRORS IN HORIZONTAL LINEAR HYDROPHONE ARRAYS IN SHALLOW WATER

by

RICHARD KLEMM

15 SEPTEMBER 1980

NORTH
ATLANTIC
TREATY
ORGANIZATION

LA SPEZIA, ITALY

Published by

INITIAL DISTRIBUTION

	Copies
MINISTRIES OF DEFENCE	
MOD Belgium	2
DND Canada	10
CHOD Denmark	8
MOD France	8
MOD Germany	15
MOD Greece	11
MOD Italy	10
MOD Netherlands	12
CHOD Norway	10
MOD Portugal	5
MOD Turkey	5
MOD U.K.	16
SECDEF U.S.	61
NATO AUTHORITIES	
Defence Planning Committee	3
NAMILCOM	2
SACLANT	10
SACLANTREPEUR	1
CINCWESTLANT/COMOCEANLANT	1
COMIBERLANT	1
CINCEASTLANT	1
COMSUBACLANT	1
COMMAIREASTLANT	1
SACEUR	2
CINCNORTH	1
CINCSOUTH	1
COMNAVSOUTH	1
COMSTRIKFORSOUTH	1
COMEDCENT	1
COMMARAIRMED	1
CINCHAN	1

	Copies
SCNR FOR SACLANTCEN	
SCNR Belgium	1
SCNR Canada	1
SCNR Denmark	1
SCNR Germany	1
SCNR Greece	1
SCNR Italy	1
SCNR Netherlands	1
SCNR Norway	1
SCNR Portugal	1
SCNR Turkey	1
SCNR U.K.	1
SCNR U.S.	2
SECGEN Rep. SCNR	1
NAMILCOM Rep. SCNR	1
NATIONAL LIAISON OFFICERS	
NLO Canada	1
NLO Denmark	1
NLO Germany	1
NLO Italy	1
NLO U.K.	1
NLO U.S.	1
NLR TO SACLANT	
NLR Belgium	1
NLR Canada	1
NLR Denmark	1
NLR Germany	1
NLR Greece	1
NLR Italy	1
NLR Netherlands	1
NLR Norway	1
NLR Portugal	1
NLR Turkey	1
NLR UK	1
NLR US	1
Total initial distribution	236
SACLANTCEN Library	10
Stock	34
Total number of copies	280

(14) SACLANTCEN [redacted]SR-46

(12)

NORTH ATLANTIC TREATY ORGANIZATION

SACLANT ASW Research Centre
Viale San Bartolomeo 400, I-19026 San Bartolomeo (SP), Italy

telex: national 0187 560940
international + 39 187 560940
telex: 271148 SACENT I

(6) A METHOD OF REDUCING BEARING ERRORS IN HORIZONTAL LINEAR HYDROPHONE ARRAYS IN SHALLOW WATER

by

(10) Richard Klemm

(11) 15 Sep[redacted]80

(12) 35

This report has been prepared as part of Project 02.

APPROVED FOR DISTRIBUTION

B.W. LYTHALL
Director

TABLE OF CONTENTS

List of Figures

A METHOD OF REDUCING BEARING ERRORS IN HORIZONTAL LINEAR HYDROPHONE ARRAYS IN SHALLOW WATER

by

Richard Klemm

ABSTRACT

Bearing estimation by means of a horizontal acoustic line array is degraded seriously by the multiple effect caused by dispersion of the field in normal modes. Error-free bearing estimates can be achieved only by means of generalized power estimators that take into account the spatial statistics (i.e. the covariance matrix) as *a priori* information about the medium. This *a priori* information is unknown in reality. It has to be substituted either by running a modelling program (e.g. normal mode) or by measurements using a test source. Measurements, however, have to be carried out for all bearings of interest. A method is suggested that uses only one test source at one known direction. The estimated test covariance function is used to calculate a beamformer matrix that can be steered in bearing. Theoretical investigations show that significant reduction of the bearing errors can be achieved.

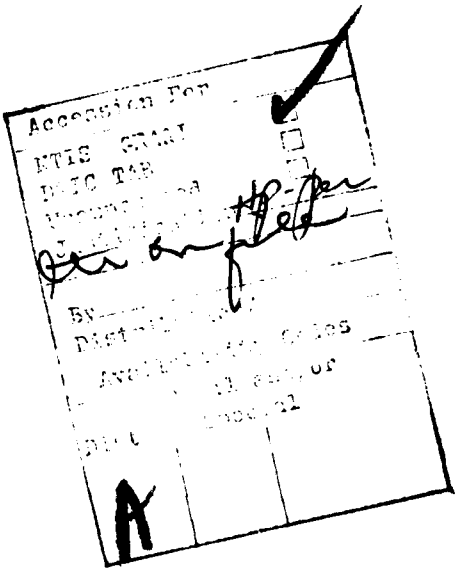

GLOSSARY

$a_a(\cdot)$	envelope of approximate spatial covariance function
$a_t(\cdot)$	envelope of spatial covariance of test signal
α	correction exponent
a_n	modal amplitudes
AMEM	approximated maximum entropy method
β	bearing angle
β_o	bearing of target
β_c	corrected bearing
β_H	look direction of steering matrix
β_t	bearing of test source
C	correlation decay factor
CBF	conventional beamformer
d	spacing between two receivers
δ	bearing error
GBF	generalized beamformer
GMLE	generalized maximum likelihood estimator
GMEM	generalized maximum entropy method
$\underline{H}(\beta)$	steering matrix
$\underline{h}(\beta)$	steering vector
k_n	modal wavenumbers
λ	wavelength
M	number of modes
MEM	maximum entropy method
MLE	maximum likelihood estimator
$\underline{N}$	noise covariance matrix
OMEM	optimum maximum entropy method

$P(\beta)$	processor output power
$\underline{p}_a$	approximated vector of phase coefficients
$P(\cdot)$	pressure
$\underline{p}_t$	vector of spatial test-signal phase coefficients
ϕ_n	modal phases
$\underline{R}$	observed covariance matrix
r	range
$\rho(\cdot)$	spatial covariance coefficient
$\rho_\phi(n,m)$	phase correlation between n^{th} and m^{th} mode
ρ_t	covariance coefficient due to pilot source test signal
$\underline{S}(\beta_o)$	spatial covariance matrix of target
$s(\beta_o)$	target signal
tr	trace of a square matrix
u	width of equivalent bearing interval
v	mid of equivalent bearing interval

INTRODUCTION

This paper presents a method of reducing the bearing errors of horizontal line arrays that may be caused by the multipath effects of sound propagating in shallow water. In a waveguide like the shallow-water channel, sound propagates in eigenfunctions of the channel (normal modes), each of them corresponding to a wavefront that is nonplanar in the vertical and arrives at a certain vertical angle at the receiver. Even if different modes are completely coherent among each other, the received wavefront is in general nonplanar also in the horizontal. If, in addition, there are phase fluctuations among modes due to some randomness of the channel the observed wavefront is random and nonplanar. In this case the signal has to be described by its spatial covariance matrix rather than by a vector of spatial field samples.

A recent theoretical study *[1]* has shown that such well-known resolution methods as conventional beamforming, maximum likelihood estimator, and maximum entropy method yield serious bearing errors for all angles other than broadside. In particular, at endfire direction the bearing offset may amount to more than 10°. In many cases more than one peak is achieved as array response to a point source. The bearing offset and the number of peaks achieved depend on the actual channel and source parameters, such as the water depth, frequency, and sound-speed profile. Furthermore, they depend on the array aperture and the resolution method used, and on the positions of source and array.

It was also shown in *[1]* that these problems can basically be overcome by use of so-called generalized resolution methods that make use of the *a priori* knowledge of the spatial statistics of the signal. These are generalized in the sense that the steering vector contained in most of the known resolution methods is replaced by a steering matrix, which is a set of spatial covariance matrices related to any expected signal. Let $\underline{R} = \underline{S}(\beta_o) + \underline{N}$ be the observed spatial covariance matrix consisting of a signal and a noise component. Then the power output of the conventional beamformer (CBF) is, in the mean,

$$P(\beta) = \underline{h}^*(\beta)\ \underline{R}\ \underline{h}(\beta), \qquad \text{(Eq. 1)}$$

where β is the bearing and $\underline{h}(\beta)$ is the steering vector with the elements $h_i = \exp(j2\pi d/\lambda \cdot i \cdot \cos\beta)$, d being the spacing between sensors. Equation 1 is optimum in the signal-to-noise ratio sense if the signal component of $\underline{R}$ is deterministic, i.e. $\underline{S} = \underline{s}(\beta_o)\ \underline{s}^*(\beta_o)$, and if $\underline{h}(\beta_o) = s(\beta_o)$, which means that the steering vector is perfectly matched to the signal wavefront. If $\underline{s}(\beta_o)$ is random the steering vector may be replaced by a steering matrix $\underline{H}(\beta)$ so that $\underline{H}(\beta_o) = \underline{S}(\beta_o)$. Hence the generalized beamformer (GBF) output power becomes

$$P(\beta) = \mathrm{tr}(\underline{R}\ \underline{H}(\beta)). \qquad \text{(Eq. 2)}$$

Similarly, the maximum likelihood estimator (MLE) *[2]*

$$P(\beta) = \underline{h}^*(\beta)\ \underline{R}^{-1}\ \underline{h}(\beta))^{-1} \qquad \text{(Eq. 3)}$$

and the maximum entropy method (MEM) *[3]*

$$P(\beta) = P_0(\underline{e}^*\underline{R}^{-1}\underline{h}(\beta)\underline{h}^*(\beta)\underline{R}^{-1}\underline{e})^{-1}, \qquad \text{(Eq. 4)}$$

with $\underline{e}^* = (1,0.....0) - j\,\underline{o}$, can be generalized to random wavefronts

$$P(\beta) = \mathrm{tr}(\underline{R}^{-1}\underline{H}(\beta))^{-1} \quad \text{(GMLE)}, \qquad \text{(Eq. 5)}$$

$$P(\beta) = P_0(\underline{e}^*\underline{R}^{-1}\underline{H}(\beta)\underline{R}^{-1}e)^{-1} \quad \text{(GMEM)}. \qquad \text{(Eq. 6)}$$

Equations 2, 5 and 6 represent the optimum resolution methods if $\underline{H}(\beta_0) = \underline{S}(\beta_0)$. We are, however, still faced with the problem that the steering matrix $\underline{H}(\beta)$ is unknown. One way of achieving a substitute for $\underline{H}(\beta)$ is to run a normal-mode program and calculate the covariance matrix of expected signals, as will be described in the next chapter. However, in this case the performance of resolution methods depends seriously on how well the predicted signal covariance fits the observed signal. In other words, the resolution depends on how far it is possible to model the actual environment. In particular, the bottom is usually unknown. Nevertheless, this method has to be investigated experimentally.

The method suggested in the following uses a pilot source with known direction to transmit a test signal. This is used to estimate the spatial response of the channel to a point source, i.e. the matrix $\underline{H}(\beta_t)$, where β_t is the direction of the test source. The problem is investigated theoretically by using a normal-mode program *[4]* to model the channel responses to the pilot source and to the target to be located.

1 THE SIGNAL MODEL

The SNAP normal-mode shallow-water sound-propagation model *[4]* gives a far-field solution of the wave equation in terms of the eigenfunctions of the acoustic waveguide

$$p(r,t) = \exp(-j\omega t) \sum_{n=1}^{M} a_n \exp(jk_n r), \qquad \text{(Eq. 7)}$$

where p is the pressure, k_n are the modal wavenumbers, and r is range. The a_n are the modal amplitudes, which depend on the positions of source and receiver and several channel properties, such as the sound-speed profile and modal attenuations. The values a_n and k_n are the output of the SNAP model *[4]* used in the following. The expressions $k_n r$ determine the modal phases between source and receiver. In order to model some randomness of the boundaries, an additional modal phase ϕ_n is introduced:

$$p(r,t) = \exp(-j\omega t) \sum_{n=1}^{M} a_n \exp[j(k_n r) + \phi_n)]. \qquad \text{(Eq. 8)}$$

This may be zero for entirely coherent modes or more or less random when modelling modal phase fluctuations. Now the spatial correlation between two points of the field r and r + d becomes

$$\rho(d) = E\{p(r,t)\ p^*(r+d,\ t)\}$$

$$= \sum_{n=1}^{M} \sum_{m=1}^{M} a_n\ a_m\ \exp\{j[(k_n - k_m)r - k_m d)]\}\ \rho_\phi(n,m), \qquad \text{(Eq. 9)}$$

where $\rho_\phi(n,m) = E\{\exp(j\phi_n)\ \exp(-j\phi_m)\}$.

For uncorrelated modes we get $\rho_\phi(n,m) = 0$, $n \neq m$, and hence

$$\rho(d) = \sum_{n=1}^{M} a_n^2\ \exp(-jk_n d). \qquad \text{(Eq. 10)}$$

In this case the field is independent of the absolute distance between source and receiver r, except for modal attenuations contained in a_n. It depends only on the spacing, d, between sensors. In particular, for a horizontal, equally-spaced array, d has to be replaced by

$$d_{ik} = (i - k)\ \cos\beta\ d_o. \qquad \text{(Eq. 11)}$$

In this case the covariance matrix across the array is Toeplitz. Except for Sect. 3.5 the following investigations are based on a signal model as

given by Eqs. 10 & 11. Additional white noise is assumed. The following parameters are kept constant if not mentioned separately:

winter sound-speed profile	as in Fig. 1a
summer sound-speed profile	as in Fig. 1b
water depth	100 m
bottom-layer depth	1 m
array depth	50 m
frequency/spacing	75 Hz / 5 m 200 Hz / 20 m 900 Hz / 50 m
signal-to-noise ratio	20 dB
number of sensors	5

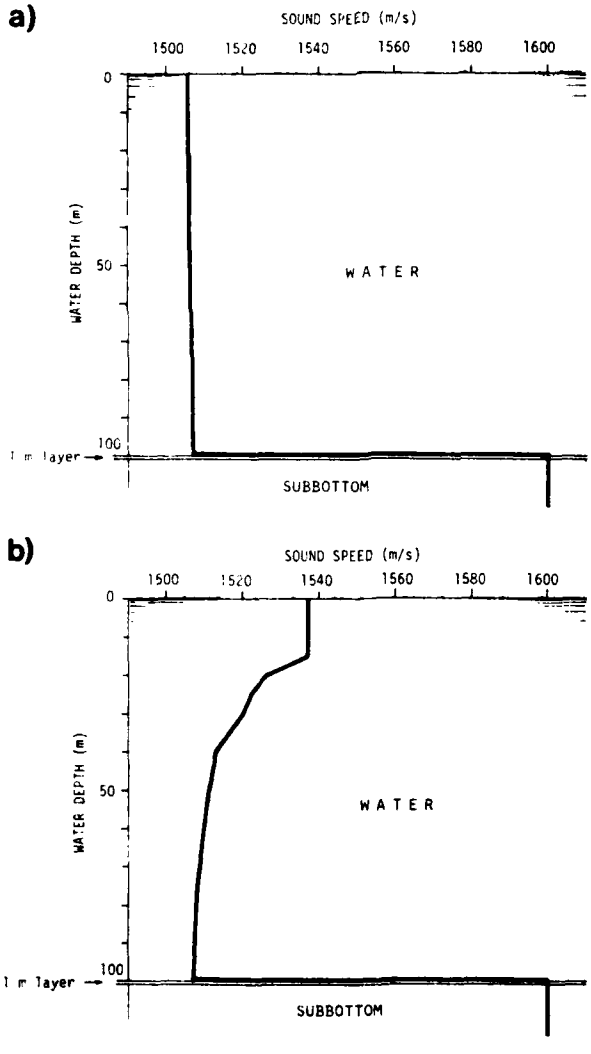

FIG. 1 SOUND-SPEED PROFILES

a) winter (SVP1)
b) summer (SVP2)

2 METHOD

Supposing a pilot source with known bearing transmitting test signals, how can the signals received by the array be used to calculate a set of steering matrices $\underline{H}(\beta)$ so as to keep bearing errors low? An obvious solution is to move the pilot source in a circle and to store test-signal covariance matrices for any bearing of interest. This involves, of course, that for any bearing of interest, e.g. every $\frac{1}{2}$ degree, the test source has to be located by other than acoustic methods, which is a tedious procedure.

The purpose of the following is to find a method for low-error bearing estimation given just one test signal arriving from the known direction β_t. The idea is to approximate the actual covariance function achieved from a test source by a covariance function of the following form:

$$p_a(i\text{-}k, \beta_t) = a_a(i\text{-}k, \beta_t)\, p_a(i\text{-}k, \beta_t), \qquad \text{(Eq. 12)}$$

where

$$a_a(i\text{-}k, \beta_t) = \operatorname{sinc}\left[\frac{2\pi}{\lambda} \cdot u \cdot d_o(i\text{-}k)\cos\beta_t\right] \qquad \text{(Eq. 13)}$$

is the envelope and

$$p_a(i\text{-}k, \beta_t) = \exp\left[j\frac{2\pi}{\lambda} \cdot v \cdot d_o(i\text{-}k)\cos\beta_t\right] \qquad \text{(Eq. 14)}$$

is the phase term. In other words, the measured test covariance function $\rho_t(i\text{-}k, \beta_t)$, describing a certain spatial distribution of the test signal, has to be approximated by a complex function of the kind of Eq. 12, which describes a spatial interval with uniform energy distribution. Thereby the unknown energy distribution of the test signal, which is characteristic for the actual state of the channel, is replaced by an equivalent angle interval of width u (difference between two directional cosines) and the mid-direction v $\cos\beta_t$). The approximation has to be carried out separately for amplitude and phase term by maximizing the generalized $\cos^2(\cdot)$ between the vectors of the test signal and those containing the terms of Eqs. 13 and 14:

$$\max_u \frac{\underline{a}_t^T \underline{a}_a \, \underline{a}_t^T \underline{a}_a}{\underline{a}_t^T \underline{a}_t \, \underline{a}_a^T \underline{a}_a} \quad \text{and} \quad \max_v \frac{\underline{p}_t^* \underline{p}_a \, \underline{p}_t^* \underline{p}_a}{\underline{p}_t^* \underline{p}_t \, \underline{p}_a^* \underline{p}_a}, \qquad \text{(Eq. 15)}$$

where $\underline{a}_t$ and $\underline{p}_t$ are the vectors of amplitudes and phase coefficients of the measured test covariance matrix and $\underline{a}_a$ and $\underline{p}_a$ are vectors containing Eqs. 13 and 14 respectively, i.e. amplitude and phase coefficients of the approximated covariance function. Maximization of expressions 15 yields the unknown parameters u and v of the equivalent angle interval with uniform energy distribution. A simple algorithm for maximizing expressions 15 is shown in Fig. 2.

The next step is to test how good the approximation is, or, in other words, how far the assumption of uniform energy distribution is valid. This is done by investigating the covariance values calculated by means of Eq. 12 and using the values u and v achieved from the approximation procedure in a square matrix $\underline{H}(\beta)$; furthermore, $\underline{H}(\beta)$ has to be inserted in one of the generalized resolution methods (Eqs. 2,5,6). If there is no difference between the known bearing of the test source and the position of the maximum obtained from the processor we conclude that the energy of the test signal is roughly uniformly distributed, i.e. the modal amplitudes a_n in Eq. 10 are equally spaced and constant for all n.

If the assumption of uniform energy distribution is not verified we get a certain bearing error by steering the approximated beamformer matrix $\underline{H}(\beta)$ over the test source; this can be used for correcting all bearings according to

$$\beta_c = \beta_H - \delta(\cos\beta_H / \cos\beta_t)^{\alpha}. \qquad \text{(Eq. 16)}$$

Here β_H is the direction at which the beamformer matrix $\underline{H}$ is looking, β_t is the bearing of the pilot source, β_c is the corrected bearing, and δ is the observed bearing error. This correction is based on the idea that as the width of the bearing interval is proportional to $\cos\beta$, the bearing error will be proportional to $\cos\beta$ as well. For instance, for the steering matrix pointing in the direction of the test source one gets $\beta_H = \beta_t$ and hence $\beta_c = \beta_H - \delta$, which is in fact the appropriate correction. The exponent α is to make the correction somewhat nonlinear in order to cope with the nonlinear distortion of the modal energy distribution for different values of β. For instance, a source located at an angle β_o that causes a certain angle interval to be uniformly covered by signal energy will never appear to be uniformly distributed at any other bearing $\beta \neq \beta_o$; this is due to the nonlinear distortion of the bearing scaling. The choice of α is not very critical; α = 5 to 15 usually yields satisfactory results. An optimum value cannot be given because it depends on the actual amplitude distribution, which depends again on the actual channel parameters.

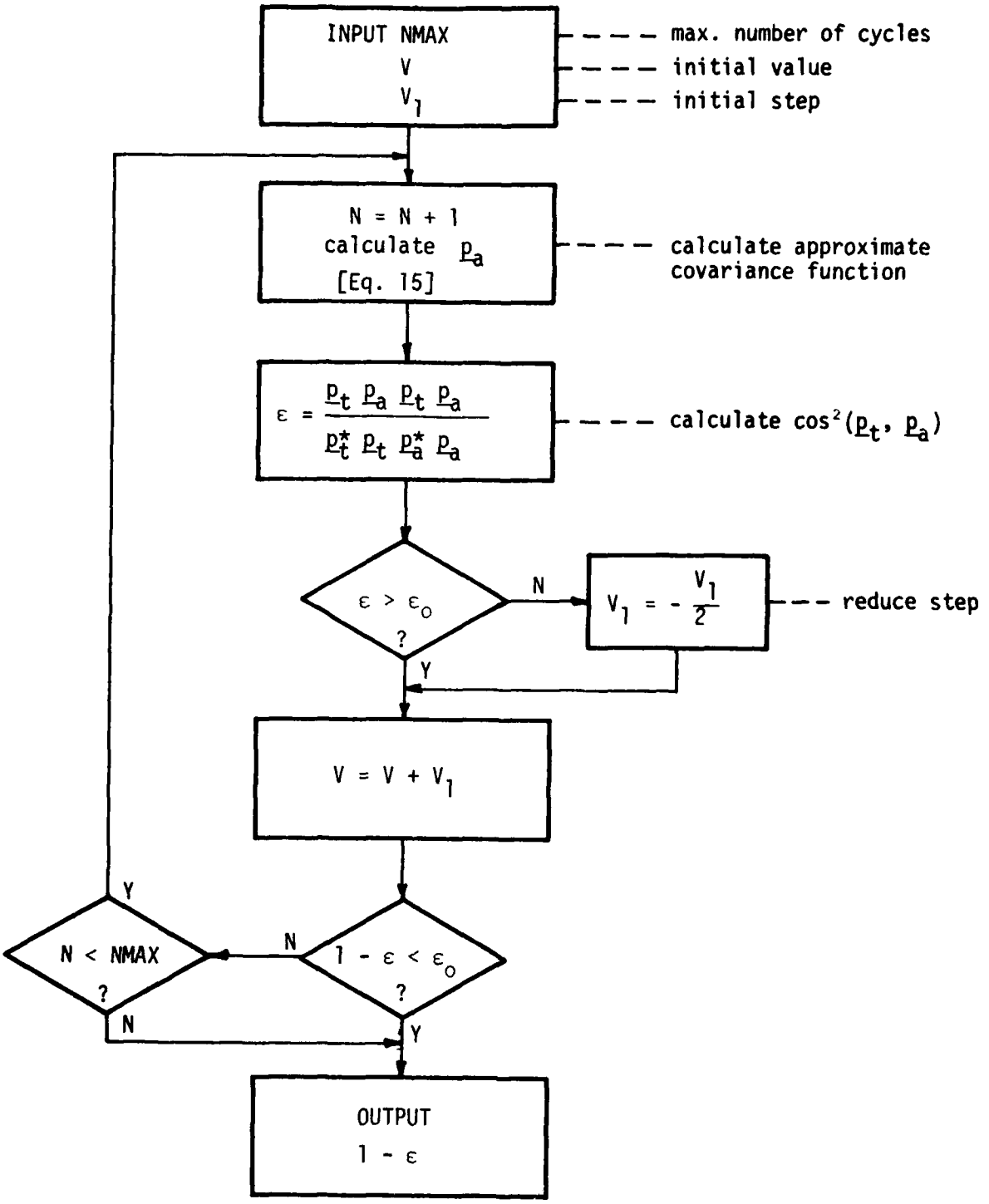

FIG. 2 THE APPROXIMATION ALGORITHM

3 NUMERICAL EXAMPLES

This chapter discusses several plots (Figs. 3 to 14) that demonstrate how the method outlined above works and what the limitations are. Throughout the examples the maximum entropy method (Eqs. 4 & 6) is used for bearing estimation. On top of each plot are two subfigures that indicate the true position ($\overset{\star}{\star}$) and the modal powers a_n^2 in logarithmic scale. The upper subfigure always denotes the pilot source used to estimate the parameters u and v (spatial spread and mean direction). The lower one represents the target source whose bearing is to be estimated. The lower one represents the target source whose bearing is to be estimated. There are always four curves. The first ("TEST") is achieved by steering the processor (Eq. 6) containing the approximated steering matrix (Eq. 12) over the test source. This curve shows how well the assumption of uniform energy distribution fits the actual channel considered. Furthermore, we get the bearing error, which is used for compensation. The OMEM (optimum maximum entropy method) curve shows the response of the processor (Eq. 6) for $\underline{H}(\beta)$, which is the exact set of signal covariance matrices as modelled by the normal-mode program, (e.g. Eqs. 9 & 10), and hence is the optimum bearing estimator. The AMEM curves (approximated maximum entropy method) represent the response of the processor (Eq. 6), with $H(\beta)$ being calculated by means of Eq. 12 using the values u, v and δ achieved from the approximation procedure of Fig. 2. Finally, the MEM curve shows the power response of the conventional maximum entropy method as given by Eq. 4.

3.1 Different Channels and Frequencies

Figures 3 to 8 show examples for several sets of parameters: the winter and summer sound-speed profiles of Fig. 1, frequencies of 75, 200, and 900 Hz, and source depths of 2, 50, and 96 m. The test source is always located at 10°, the target at 20°.

The first impression is that the conventional MEM yields high resolution, but, in most cases gives considerable bearing errors. In particular, the MEM attempts to resolve the internal structure of the channel response to the source, which is not very meaningful for source location. In some cases single modes are resolved (e.g. Fig. 3b). The optimum method (OMEM) points always at the true target position, as expected. The method suggested in this paper sometimes achieves the right bearing (Figs. 4a, 8a); in all other cases bearing errors of 0.5° to 1.5° are observed. It is noticed that, except for a few examples (Figs. 3a, 3c, 6a, 7a), the bearing estimate is upward biased, i.e. the bearing estimate is higher than the true bearing of the target. The reason is that in these examples the bearing error is slightly over-compensated by the term of Eq. 16. This offset can be reduced by choosing the exponent α to be of a higher value. In the examples of Figs. 3 to 8 we have chosen $\alpha = 5$. The choice $\alpha = 10$ to 15 would yield even better results on the average than those presented here.

Apart from the fact that in most of the examples presented here the conventional resolution method (MEM) yields two peaks instead of one, we observe that there is almost no example indicating that under certain conditions the MEM is superior to the AMEM (compare the bearing of the highest peak of the MEM curves with the AMEM response). Only in Fig. 3b is the bearing of the higher MEM peak closer to the true bearing than the AMEM. There are, however, several examples (e.g. Figs. 3a, 3c, 6a, 7a, 8a) that show a significant improvement of the bearing estimate achieved by the AMEM. The AMEM is superior in particular if the major part of the energy is in the higher order modes, which happens if the source is close to the surface (e.g. Figs. 3a, 3c, 7a, 8a).

3.2 Aperture

Figure 9 uses the example shown in Fig. 8a to investigate the upper limit of resolution of the AMEM. Different plots show the responses of arrays with increasing spacing (2, 4, 8, 12 m), corresponding to 1.19, 2.38, 4.76, 7.14λ. There are always five sensors.

Figure 9a shows that (for the example chosen) up to a 6λ aperture the AMEM is identical to the optimum processor (OMEM). The maximum resolution achievable is given by using a 12λ aperture (Fig. 9b). A slight difference between OMEM and AMEM response can be noticed. Doubling the spacing once more to 24λ (Fig. 9c) yields already a considerable degradation of resolution and deviation from the OMEM response. The first grating lobes can be seen on the right.

Figure 8d shows the performance of an array with a 36λ aperture. It can be recognized, in particular, that contrary to the examples discussed before, the TEST curve (steering the uncorrected processor over the pilot source) is completely offset. Consequently the corrected AMEM processor also points in the wrong direction. The reason for this behaviour is simply that the approximation algorithm (Fig. 2) did not converge properly, which may of course lead to any erroneous result. If the approximation has failed, no reasonable result can be expected from the AMEM.

As a conclusion, we should first keep in mind that resolution is always limited by any lack of *a priori* knowledge about the signal to be resolved. According to the performance of the AMEM this means that the resolution achieved depends on how the measured covariance function can be approximated by the complex sinc-function (Eq. 13). Obviously, the approximation works better for small apertures than for larger ones; hence there is a natural limit for resolution. Further, we can say that a generalized beamformer-type processor (Eq. 2) using the approximation procedure to calculate $\underline{H}(\beta)$ is not at all applicable for bearing estimation because it needs a very large aperture in order to achieve resolution comparable to the adaptive methods (MLE, MEM), which prevents convergence of the approximation algorithm.

As it turns out that the approximation procedure is limited to rather small apertures (about 12λ) the general policy should be to use a large array and conventional or adaptive beamforming, or any other kind of detection scheme

[5] based on the CBF that maximizes the signal-to-noise ratio in order to detect targets from noisy background. As a second step, only a small part of the array should be used for bearing estimation using the AMEM.

3.3 Position of Pilot Source and Target

This section looks at the questions of whether there is a preferable pilot-source position and if one pilot source at one known bearing is sufficient to model the steering matrix $\underline{H}(\beta)$ for the whole bearing range of interest.

Figure 10 shows the same examples as before, but with the pilot source being moved around. As can be seen, the bearing estimate is quite independent of the position of the test source. Of course, for bearing angles close to 90° (broadside) no good estimates can be expected for the values u and v in Eqs. 12, 13 and 14, because the angle interval of signal arrivals approaches zero. The method seems also to be very insensitive to any change in target position, as seen in Fig. 11.

Figure 12 shows two examples in which the pilot source is located at endfire direction. The examples chosen are the same as in Figs. 7a and 7c, except that instead of the pilot source being at 10° it is here at endfire. It is seen that in Fig. 12a the AMEM is as good as it was in Fig. 7a. Figure 12b, however, shows that there are some situations in which the endfire position is not useful for positioning the pilot source, Fig. 7c showing a much better bearing estimate. This can be explained by the spatial aliasing effect at endfire. The channel response to a source close to endfire is corrupted by its reflected image about the value of $\beta = 0°$. This aliased signal response is in many cases useless for predicting the spatial spread and mean direction of a source at angles different from endfire and, hence, much less aliased.

3.4 Mismatch in Depth

So far it has been assumed that the depths of the test-source and the target are the same. In the two examples in Fig. 13a & b it is assumed that the target is at 2 m depth and that the pilot source is at 30 m and 50 m depths respectively. Except for the changes in pilot source depth, these examples are the same as that given in Fig. 7a. These examples show that there can be considerable differences in energy distribution between test signal and target. In some instances it may happen that the bearing estimate is corrupted seriously by mismatch between pilot-source response and response to the target, as shown in Fig. 13a. In other instances, such as in Fig. 13b, a good estimate is achieved although the spatial characteristics are quite different. A general statement about the sensitivity to mismatch in depth between pilot source and target cannot be made. Therefore, if possible, the pilot source should be kept at the target depth of interest.

3.5 Correlation among Modes

So far it was assumed that modes are uncorrelated among each other, i.e.

$$E\{e^{j\phi_n} e^{-j\phi_m}\} = 1 \quad n = m$$
$$= 0 \quad n \neq m.$$

In this case wavefronts are random, non-planar, and range independent in the mean. The spatial covariance matrix is Toeplitz and, hence, the best match between the approximation method and the field is achieved because the steering matrix $\underline{H}(\beta)$, as calculated by Eqs. 12, 13 and 14, is Toeplitz.

If, however, there is some correlation between modes the field becomes range independent and the covariance matrix non-Toeplitz. If, for instance, $E\{e^{j\phi_n} e^{-j\phi_m}\} = 1$ for all n,m one receives non-random non-planar wavefronts whose shapes depend on the distance between source and receiver. Therefore it can be expected that the resolution of any processor (except for the OMEM, which contains *a priori* knowledge about the modal amplitudes and phases) is degraded due to mismatch to the field (mismatch of the steering vector as suboptimum steering matrix to non-planar wavefronts).

In other words, if the modes are uncorrelated, i.e. phase among modes are entirely random, then the signal energy is distributed in the mean as shown in the subfigures of the plots. If modes are correlated, the shapes of the wavefronts are distorted additionally by mode interference, which may cause a significant deviation from a rectangular energy distribution that the AMEM is based on. As a consequence, the signal field cannot be approximated sufficiently well by the sinc-function (Eqs. 12, 13 & 14), thus causing additional mismatch between the AMEM processor and the signal field.

We use the following correlation model

$$\rho_\phi(n,m) = \rho_o(n,m) \qquad \rho_o(n,m) > 0$$
$$= 0 \qquad \rho_o(n,m) < 0, \qquad \text{(Eq. 17)}$$

where

$$\rho_o(n,m) = 1 - \frac{C|n-m|}{M} .$$

For C = 0 we get $\rho_o(n,m) = 1$, i.e. modes are entirely correlated, C > M yields uncorrelated modes. Some results are shown in Fig. 14. It can be seen that for C = 1 (Fig. 14a) (triangular correlation among modes) rather high resolution is achieved. The AMEM obviously gives a rather good bearing estimate (0.5° offset). The correlation is still weak enough for appropriate approximation of the signal covariance matrix by the sinc-function of Eq. 12. For C = 0.1 (Fig. 14b) the correlation function is a triangle on a pedestal of 0.9 height. A considerable loss in resolution is observed and the mismatch of the steering matrix (in the case of the AMEM) or the conventional beamformer (in the case of MEM) now becomes significant. With total correlation (C = 0, Fig. 14c) the resolution achieved is even worse (except for the OMEM, which is perfectly matched in any case). However, in all cases considered, the AMEM appears to be superior to the conventional MEM.

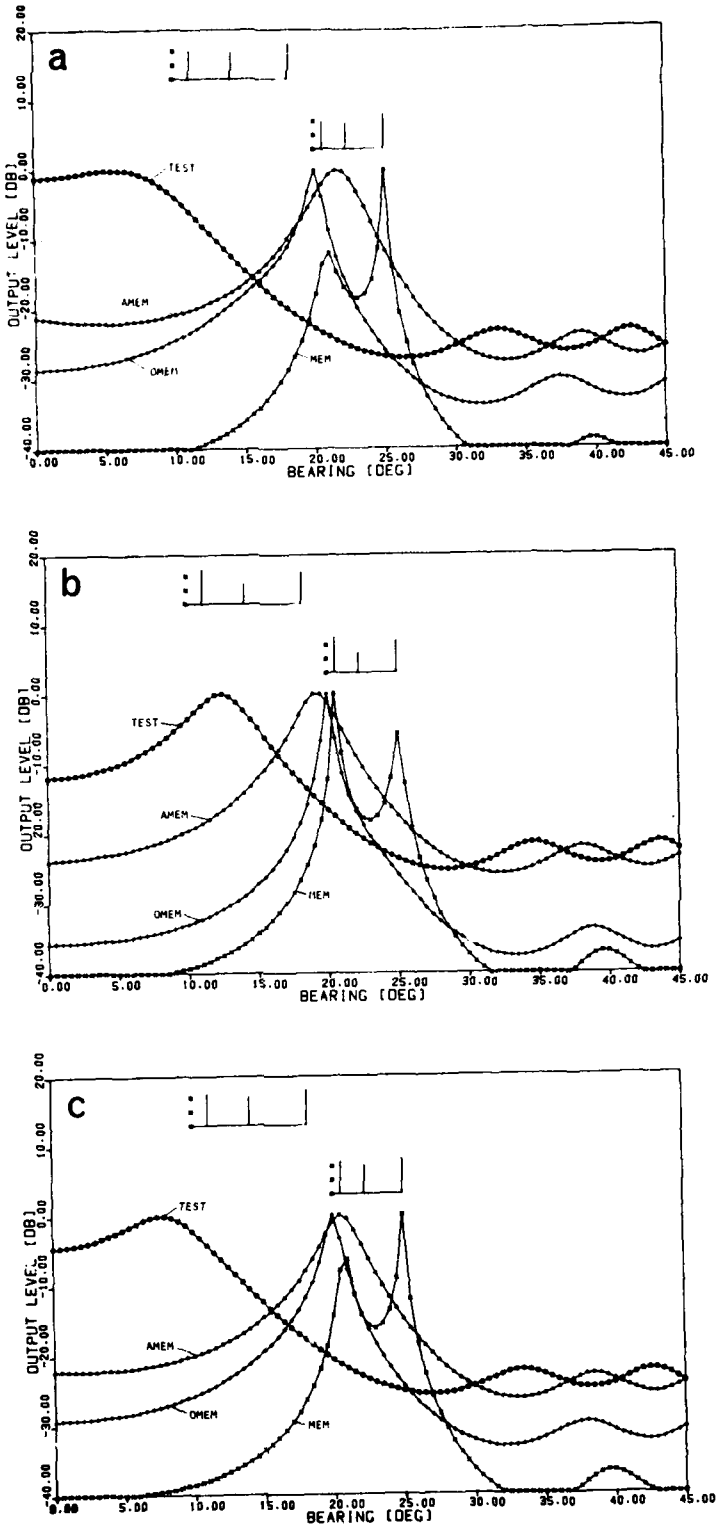

FIG. 3 EXAMPLES FOR 75 Hz AND WINTER SOUND-SPEED PROFILE

a) 2 m pilot-source depth
b) 50 m pilot-source depth
c) 96 m pilot-source depth

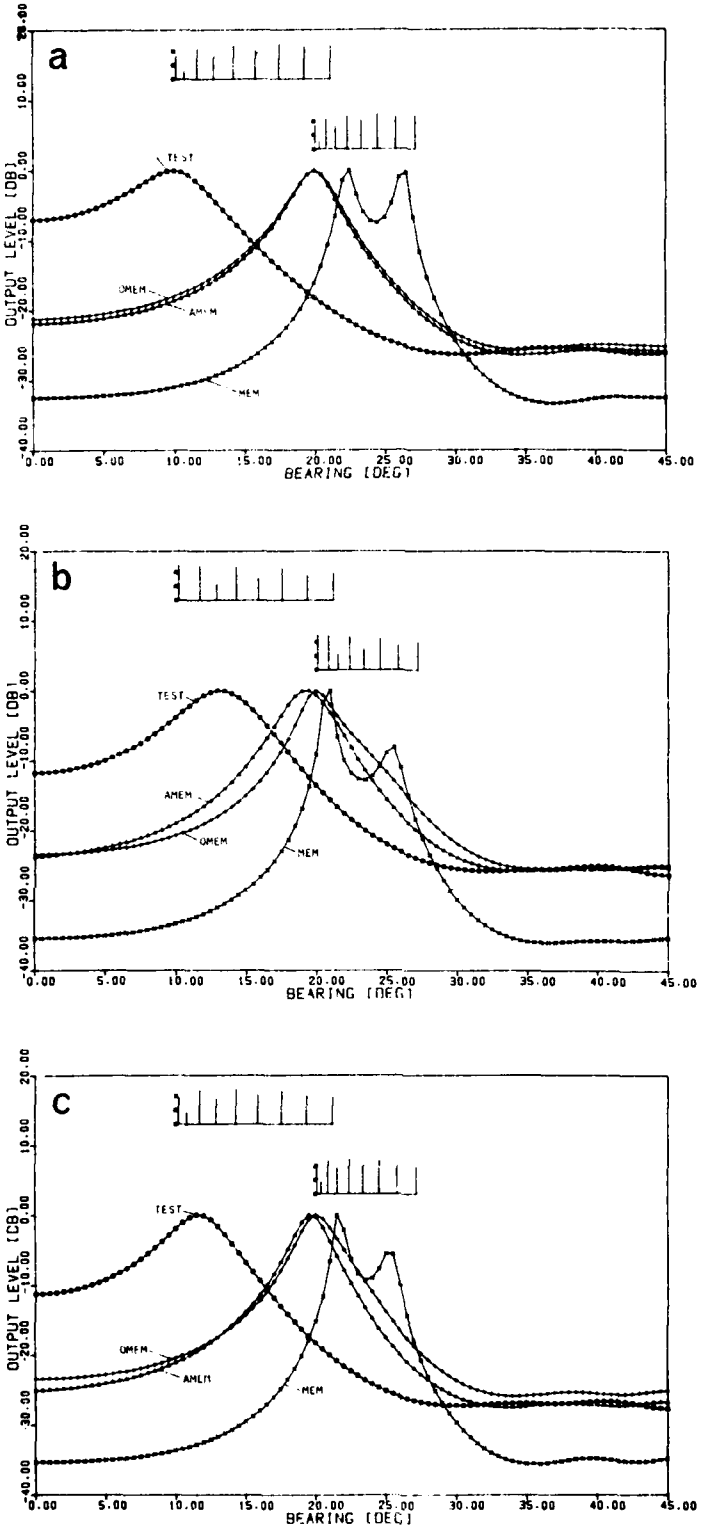

FIG. 4 EXAMPLES FOR 200 Hz AND WINTER SOUND-SPEED PROFILE

a) 2 m pilot-source depth
b) 50 m pilot-source depth
c) 96 m pilot-source depth

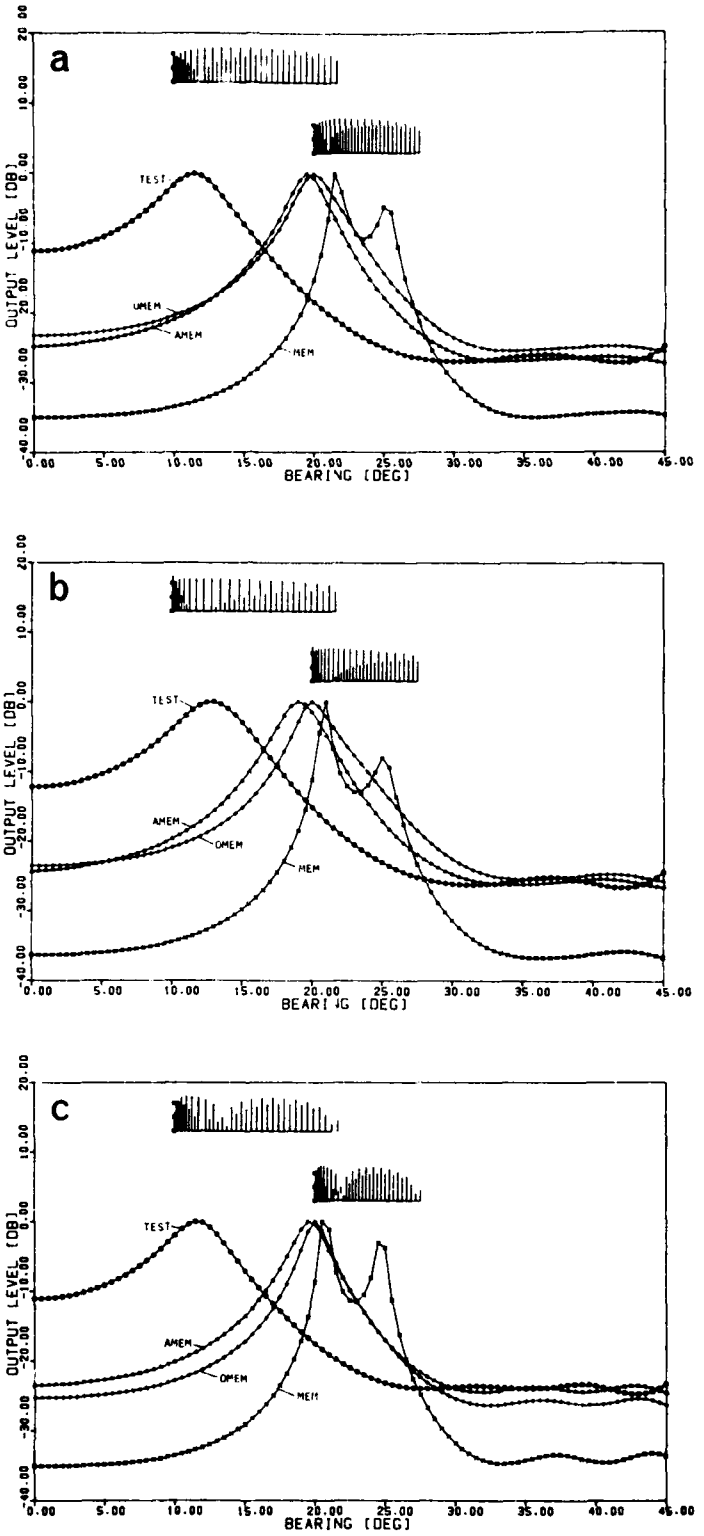

FIG. 5 EXAMPLES FOR 900 Hz AND WINTER SOUND-SPEED PROFILE

a) 2 m pilot-source depth
b) 50 m pilot-source depth
c) 96 m pilot-source depth

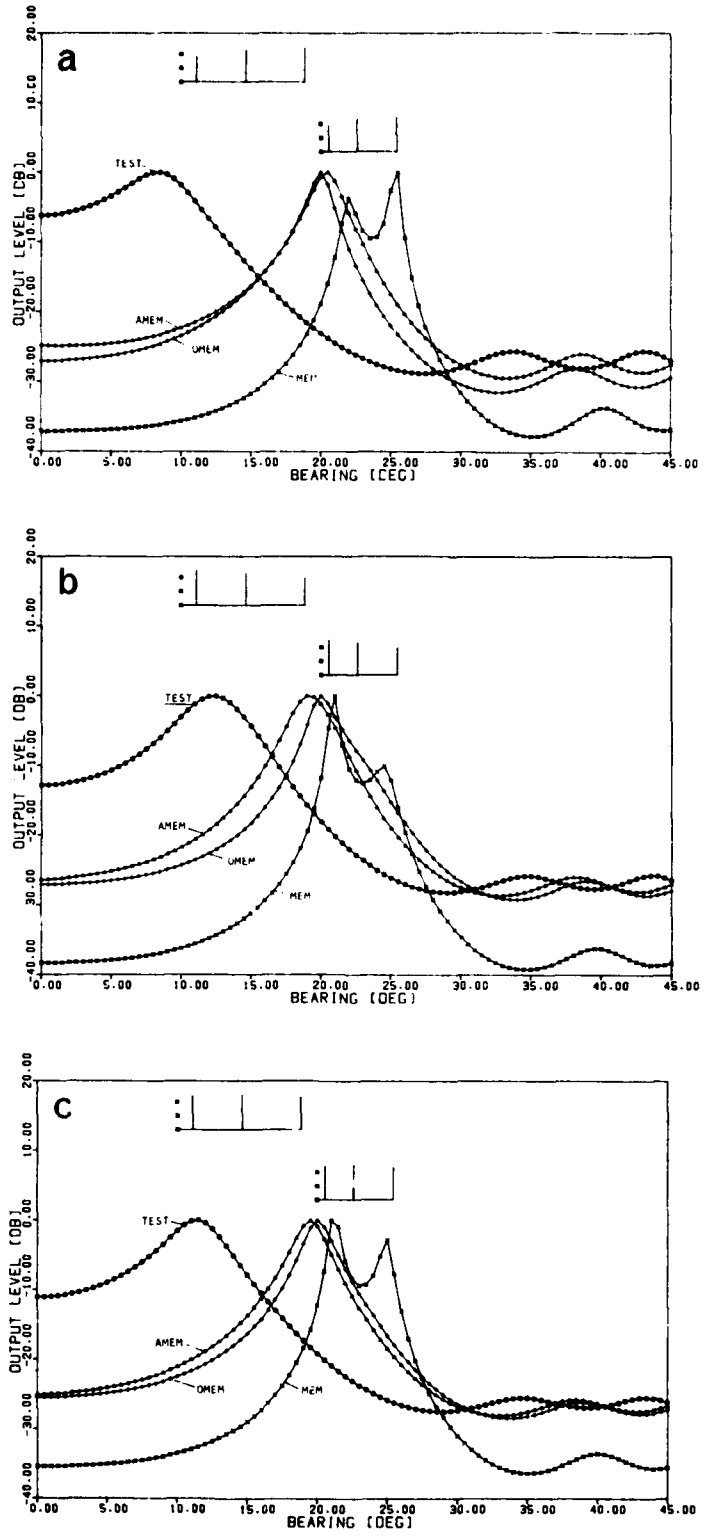

FIG. 6 EXAMPLES FOR 75 Hz AND SUMMER SOUND-SPEED PROFILE

a) 2 m pilot-source depth
b) 50 m pilot-source depth
c) 96 m pilot-source depth

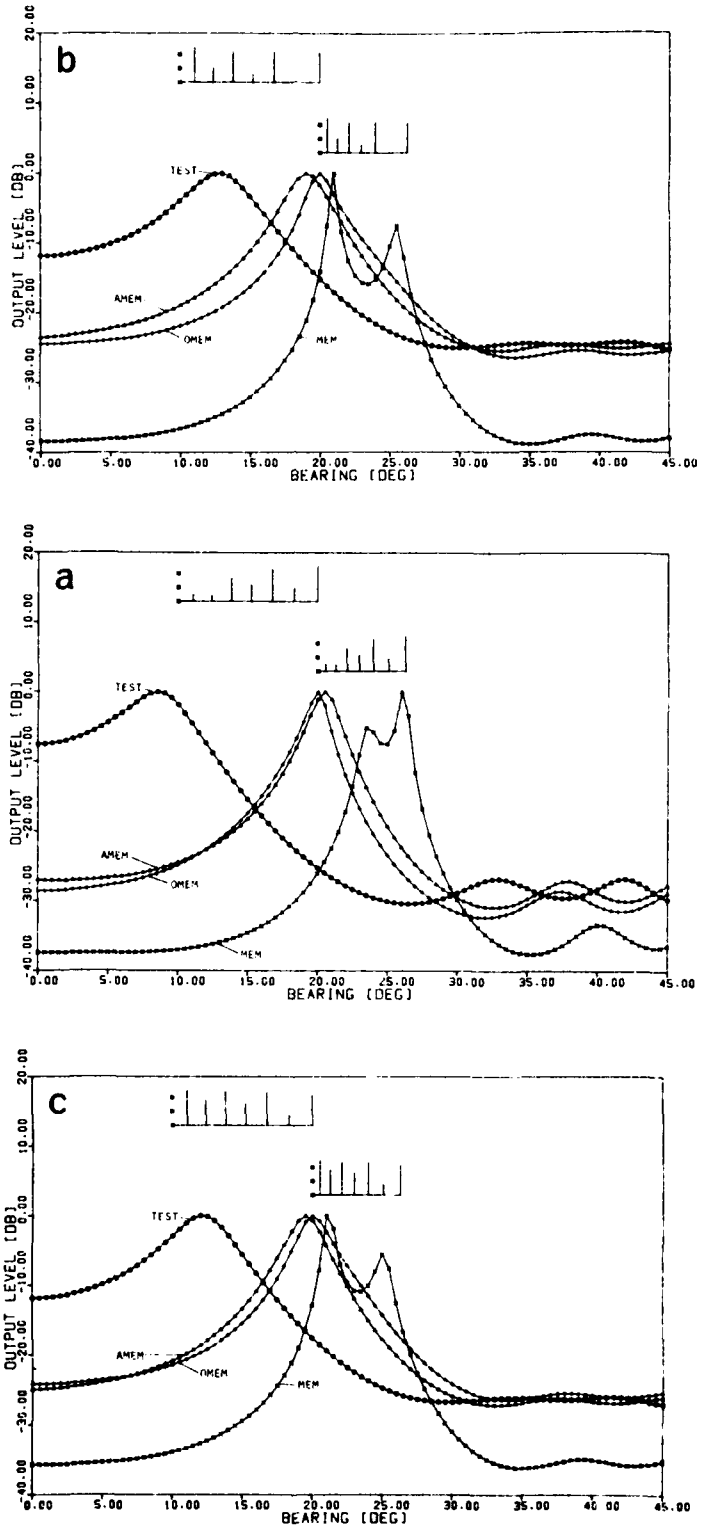

FIG. 7 EXAMPLES FOR 200 Hz AND SUMMER SOUND-SPEED PROFILE

a) 2 m pilot-source depth
b) 50 m pilot-source depth
c) 96 m pilot-source depth

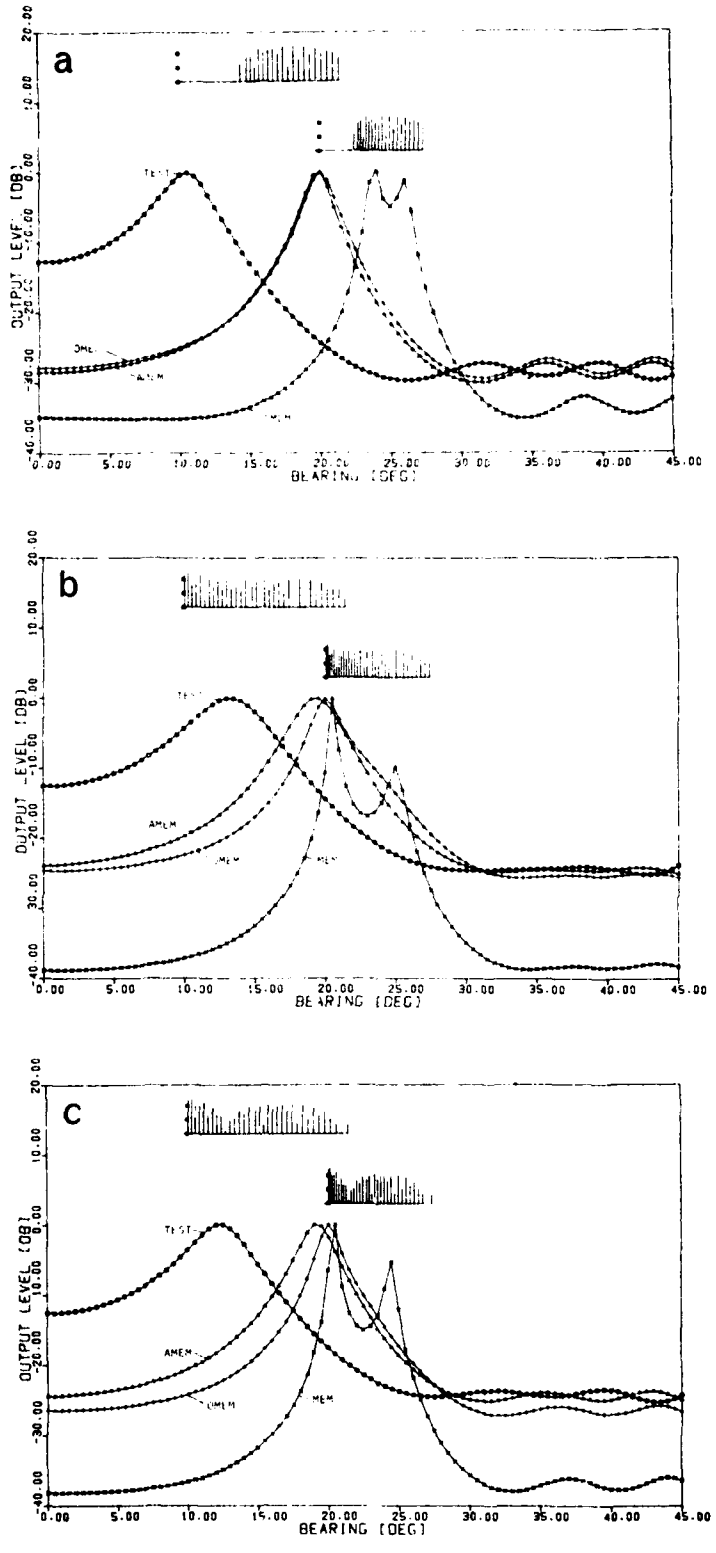

FIG. 8 EXAMPLES FOR 900 Hz AND SUMMER SOUND-SPEED PROFILE

a) 2 m pilot-source depth
b) 50 m pilot-source depth
c) 96 m pilot-source depth

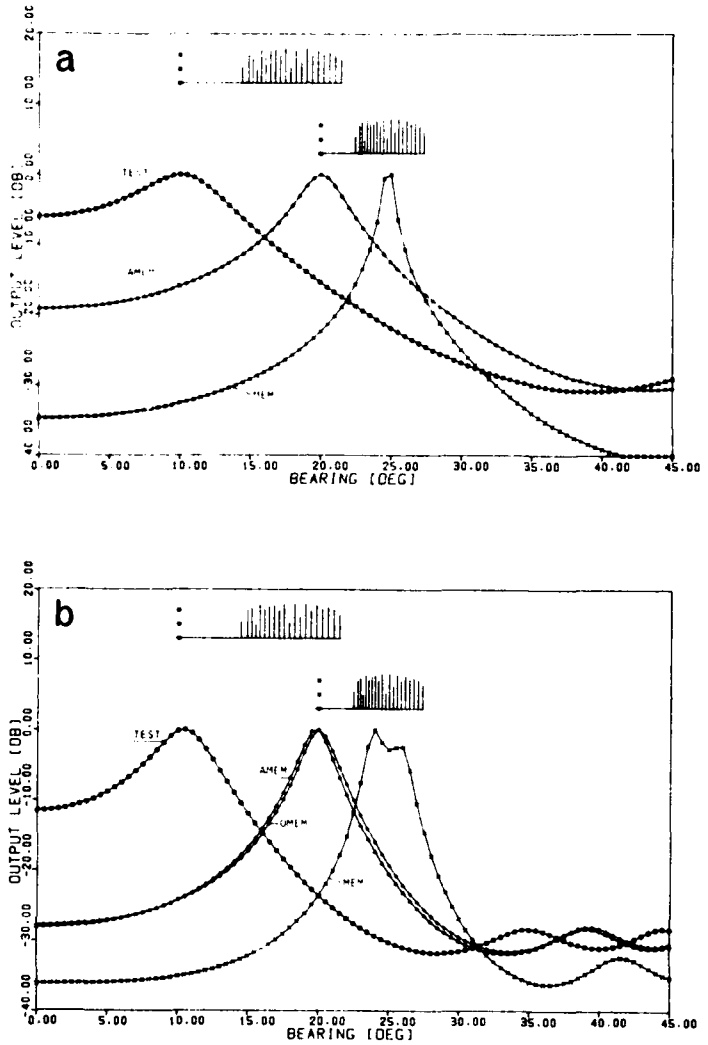

FIG. 9 EXAMPLE OF FIG. 8a BUT WITH DIFFERENT ARRAY SPACINGS:

a) 2 m pilot-source depth
b) 4 m pilot-source depth

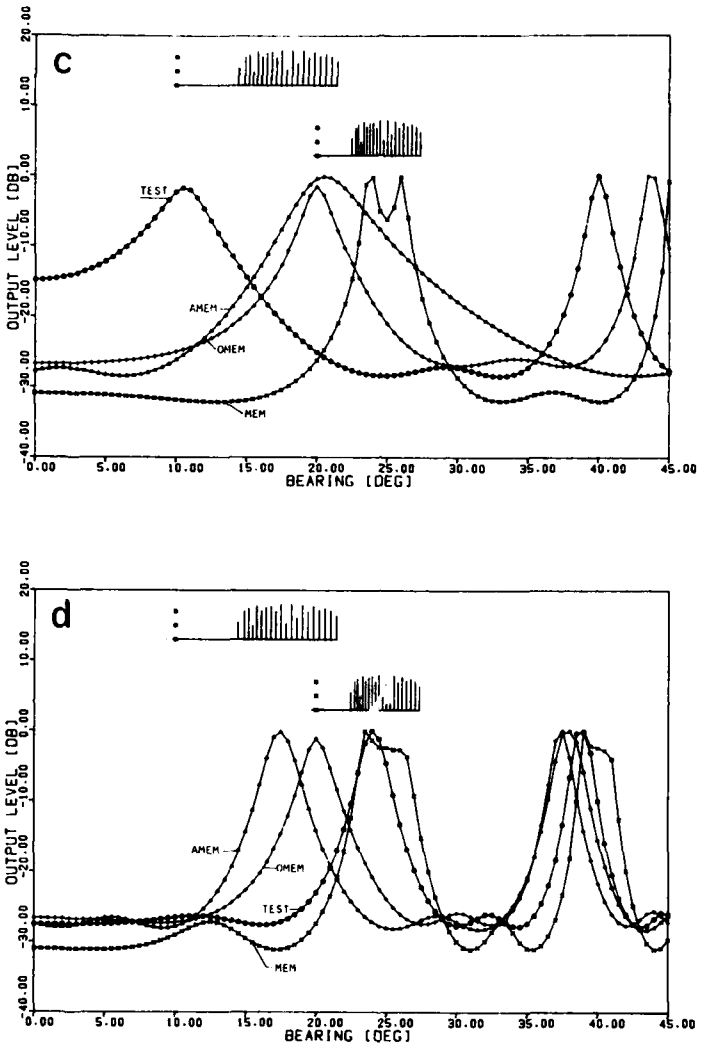

FIG. 9 EXAMPLE OF FIG. 8a BUT WITH DIFFERENT ARRAY SPACINGS

c) 8 m pilot-source depth
d) 12 m pilot-source depth

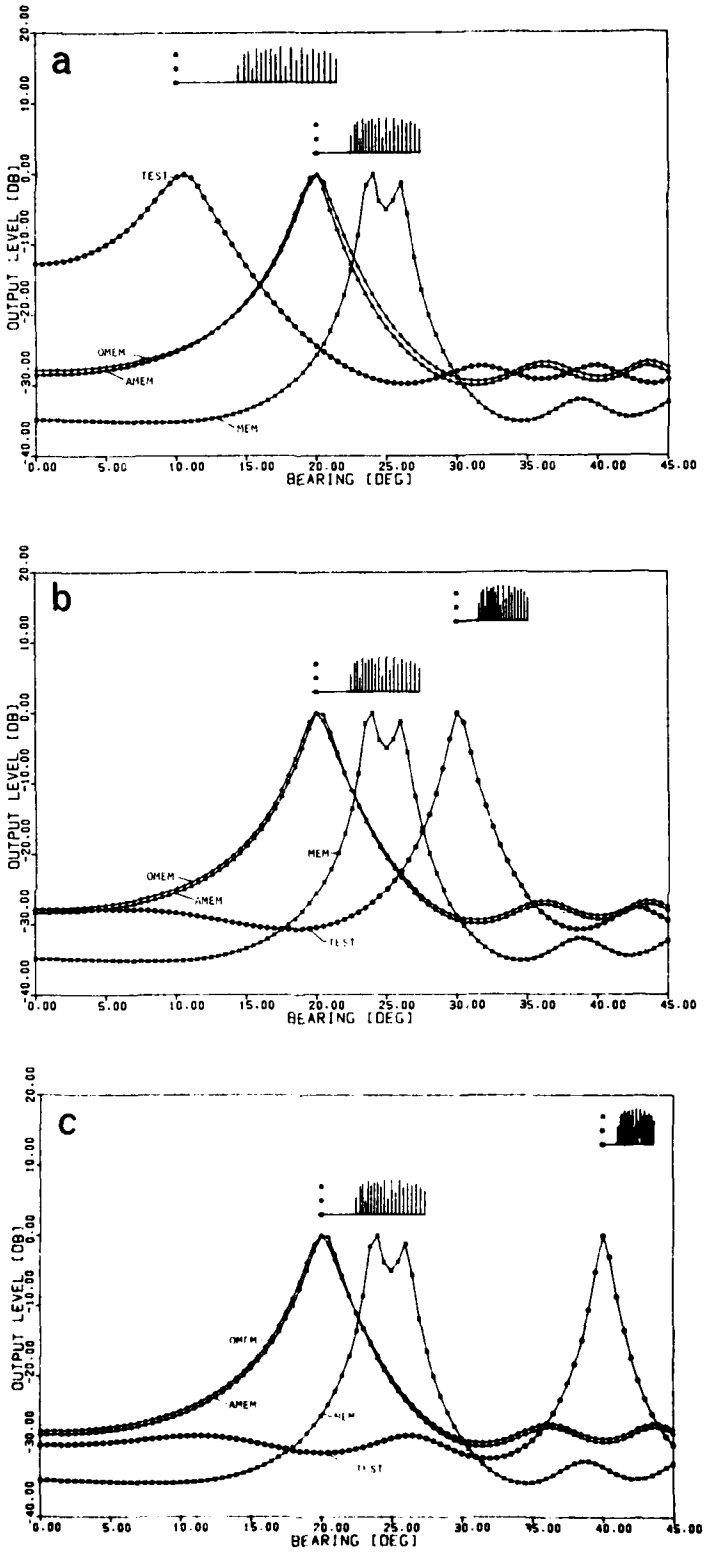

FIG. 10 EXAMPLE OF FIG. 8a BUT WITH CHANGES IN THE BEARING OF THE PILOT SOURCE:

a) 2 m pilot-source depth
b) 50 m pilot-source depth
c) 96 m pilot-source depth

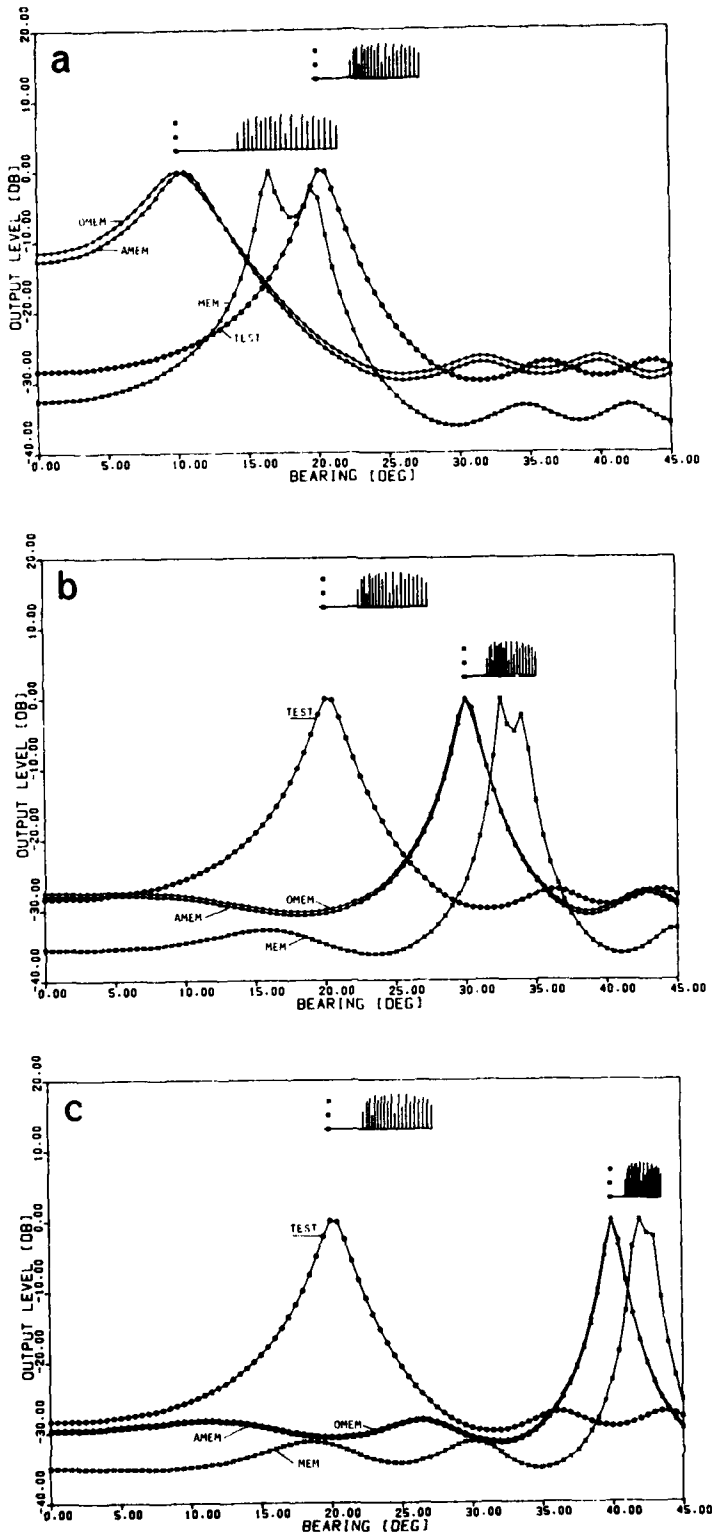

FIG. 11 EXAMPLE OF FIG. 8 BUT WITH CHANGES IN THE BEARING OF THE TARGET

a) 2 m pilot-source depth
b) 50 m pilot-source depth
c) 96 m pilot-source depth

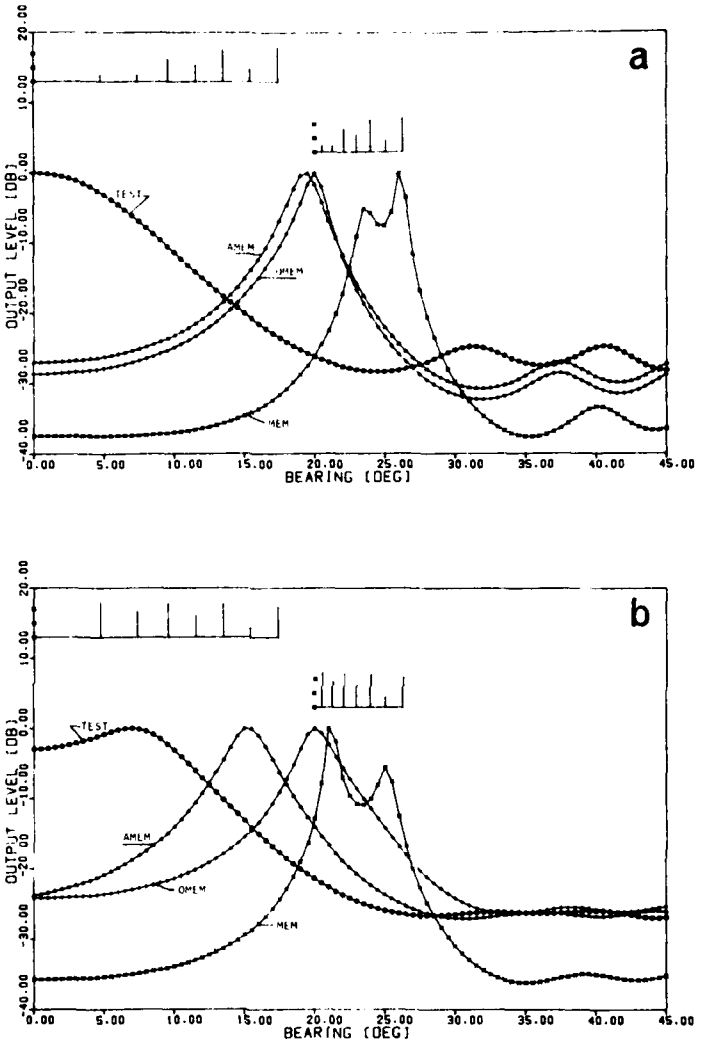

FIG. 12 EXAMPLES WITH THE PILOT SOURCE AT ENDFIRE (200 Hz, SUMMER PROFILE)

a) 2 m pilot-source depth
b) 96 m pilot-source depth

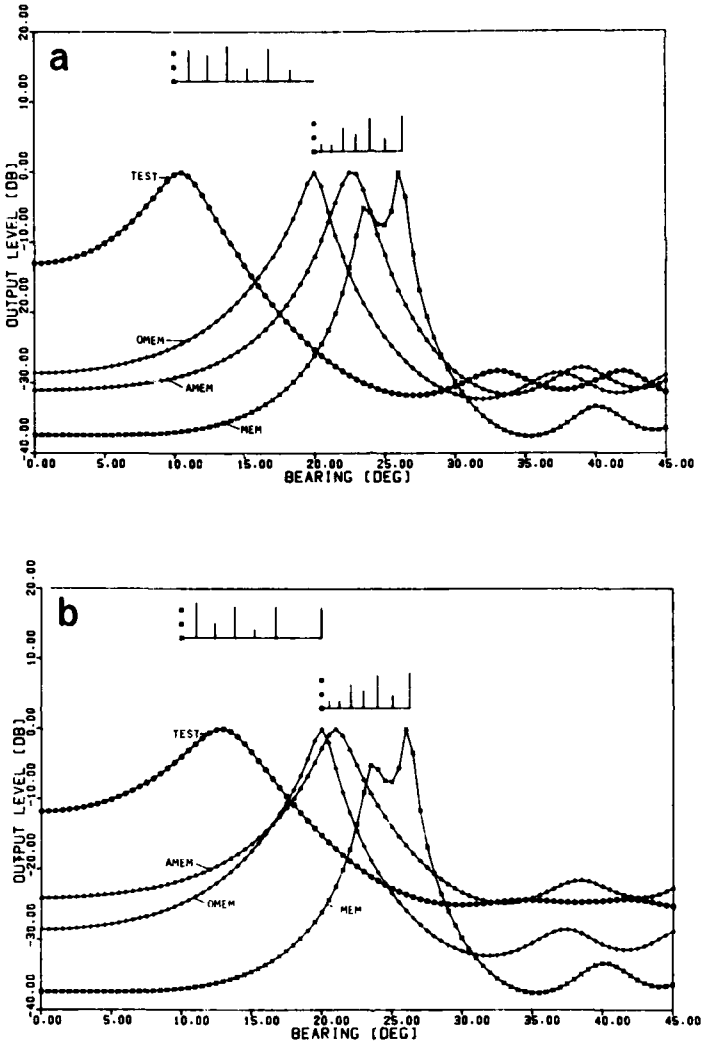

FIG. 13 EXAMPLES WHERE PILOT SOURCE AND TARGET ARE NOT AT THE SAME DEPTH

a) source at 2 m, target at 30 m
b) source at 2 m, target at 50 m

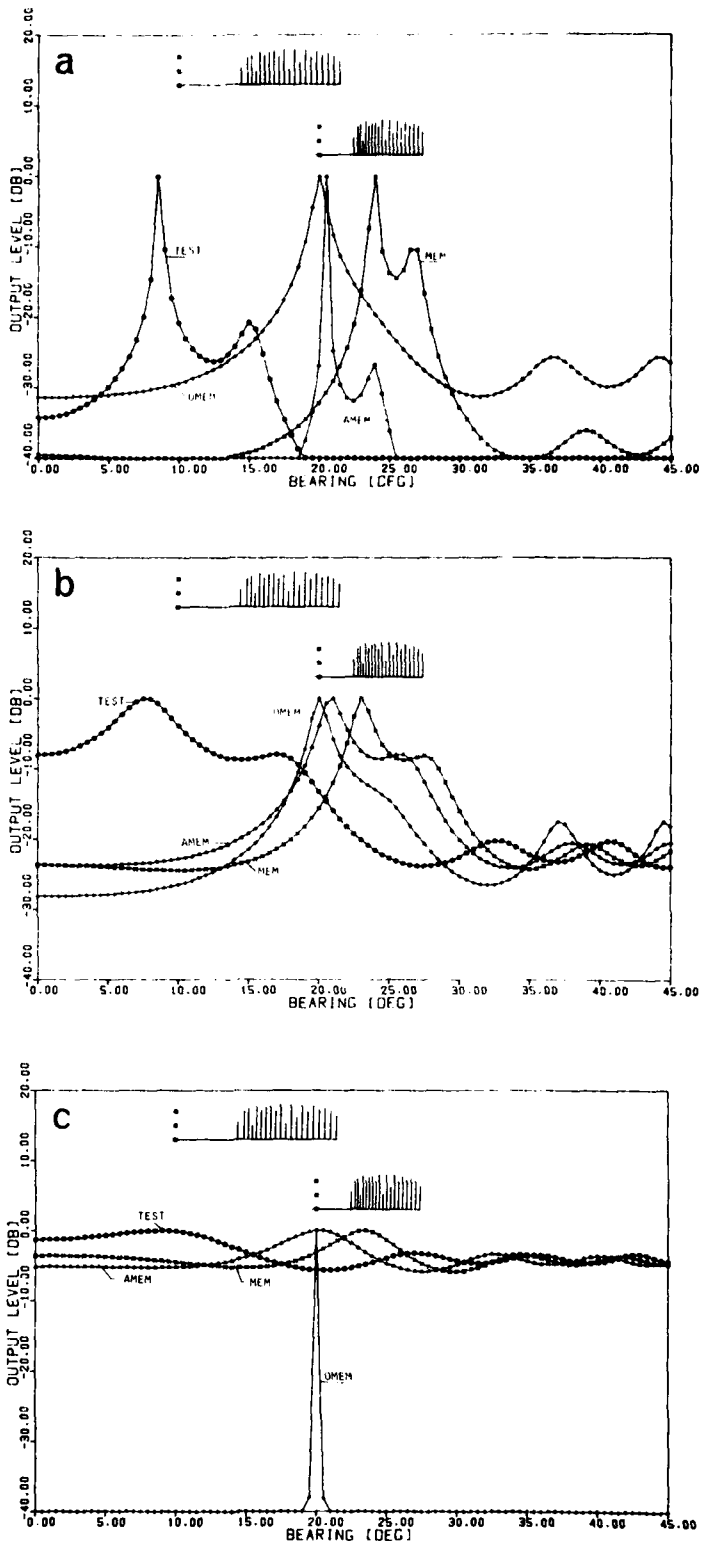

FIG. 14 EXAMPLES OF DIFFERENT CORRELATION BETWEEN MODES

a) triangular correlation (C = 1)
b) correlation of C = 0.1
c) total correlation (C = 0)

CONCLUSIONS

A method (AMEM) has been described to reduce the bearing error of horizontal line arrays caused by multipath effects of sound propagating in shallow water. The procedure consists of the following steps:

1. Use a pilot source of a certain known bearing angle between 10° and 45° (0° = endfire) or 135° and 170° and estimate the spatial correlation coefficients for all delays of the array, i.e. ρ_{11}, ρ_{12},$\cdots\rho_{1N}$.

2. Approximate the measured correlation function by a sinc(•)exp(j(•))-function (Eqs. 12, 13 & 14) using the algorithm of Fig. 2 and achieve the values u (width of equivalent angle interval) and v (mid direction).

3. Calculate steering matrices $\underline{H}(\beta)$ by means of Eqs. 12, 13 & 14 using the estimated values of u and v.

4. Insert $\underline{H}(\beta)$ in a high resolution method (Eqs. 5 & 6), preferably, steer the processor over the pilot source, and determine what bearing error is characteristic of the existing channel conditions.

5. Use the bearing error δ for bearing correction of $H(\beta)$ by means of Eq. 16.

6. If there is some directional noise present when the steering matrix is being updated, then

   a. estimate spatial noise covariance function n_{11},$n_{12}\cdots n_{1N}$, when no test signal is present,

   b. estimate the spatial covariance function r_{11},r_{12},$\cdots r_{1N}$, when signal and noise are present,

   c. subtract the noise component from the measured covariance function $\rho_{11} = r_{11}-n_{11}$, $\rho_{12} = r_{12}-n_{12}$, $\rho_{1N} = r_{1N}-n_{1N}$.

The method has been investigated numerically by application to a normal-mode sound-propagation model, assuming that modes are uncorrelated. The results can be summarized as follows:

a. The AMEM response to a point source is usually one peak in bearing. Conventional resolution methods like MEM or MLM may yield a thousand or more peaks, depending on the spatial energy distribution of the signal and the aperture of the array.

b. The method has been tested for different conditions of the channel (two sound-speed profiles, three frequencies, three source depths). In most cases observed, the maximum of the AMEM-response was closer to the true bearing of the target than the maximum peak determined by the MEM.

c. The maximum aperture to be used is about 12λ. Beyond 12λ the algorithm of Fig. 2 does not converge sufficiently well, thus causing a mismatch between steering matrix and field that leads to degradation of resolution.

d. The method is useful for bearing-error reduction for targets located between 10° and 170°. Targets at about 90° (broadside) do not of course need to be corrected. At endfire direction (0° to 10°) the method is, in many cases, corrupted by spatial aliasing and should be used carefully.

e. The pilot source should be located at angles between 10° and 45°. The accuracy of the AMEM depends, of course, on how precisely the position of the pilot is known.

f. The AMEM (or AMLM) is superior to conventional adaptive methods (MEM, MLM), particularly if the major part of the energy is contained in the higher-order modes, i.e. for a source located close to the surface or to the bottom.

g. Even if the field is inhomogeneous due to mode interference the AMEM seems to be superior to the conventional methods.

h. The sinc-function seems to be an appropriate way of approximating the envelope of the covariance function because the assumption of uniform energy distribution is available. Nevertheless, in certain cases, other functions might be even better, which can always be judged by consideration of the approximation error $1-\varepsilon$ in the algorithm of Fig. 2. Of course, whatever function is used, it has to be one that depends only on $u \cdot \cos\beta$ in order to adjust it to the interval width varying with bearing.

i. The AMEM is basically sensitive to mismatch between pilot-source depth and target depth. Therefore the pilot source should be located at the depth of interest for target location.

j. The method outlined above is adaptive in that it allows the steering matrix to be updated with changing environmental conditions.

k. Basically, the method is based on the assumption that there are phase fluctuations among modes, which is supposed to be valid for higher frequencies rather than for lower ones. The validity of this assumption has to be proved experimentally.

REFERENCES

1. KLEMM, R. On the use of generalized resolution methods to locate sources in random dispersive media. IEE Proceedings 127F, 1, 1980: 34-40.

2. COX, H. Resolving power and sensitivity to mismatch of optimum array processors. J. Acoustical Society America 54, 3, 771-785.

3. BURG, J.P. A new analysis technique for time series data. In: NATO Advanced Study Institute on Signal Processing with Emphasis on Underwater Acoustics, Enschede, 1968, Proceedings, volume 1. Enschede, Twente Institute of Technology, 1968: 15-1 to 15-7.

4. JENSEN, F.B., FERLA, M.C. SNAP: The SACLANTCEN normal-mode acoustic propagation model, SACLANTCEN SM-121. La Spezia, Italy, SACLANT ASW Research Centre, 1979. [AD A 067 256]

5. KLEMM, R. Detection performance of horizontal linear hydrophone arrays in shallow water. SACLANTCEN SR- in preparation.